

Spatial, Polarization, and Pattern Diversity for Wireless Handheld Terminals

Carl B. Dietrich, Jr., *Member, IEEE*, Kai Dietze, J. Randall Nealy, and Warren L. Stutzman, *Fellow, IEEE*

Abstract—This paper examines the antenna diversity configurations that improve performance in handheld radios. Experiments using spatial, polarization, and pattern diversity were conducted for both line-of-sight (LOS) and obstructed outdoor and indoor multipath channels that experienced Ricean fading. Antenna separation, polarization, and pattern were varied independently to the extent possible. Envelope correlation, power imbalance, and diversity gain were calculated from the measurements. Diversity performance is measured by diversity gain, which is the difference in signal-to-noise ratio (SNR) between the output of a diversity combiner and the signal on a single branch, measured at a given probability level. Diversity gain increases with decreasing envelope correlation between the antenna diversity branches. However, diversity gain decreases as power imbalance between diversity branches increases because a branch that has a weak signal has only a small contribution to the combined signal. Diversity gain values of 7–9 dB at the 99% reliability level were achieved in non-line-of-sight (NLOS) channels for all diversity configurations even with very small antenna spacings. The use of polarization diversity reduced polarization mismatches, improving SNR by up to 12 dB even in LOS channels.

Index Terms—Antenna diversity, handheld wireless communication.

I. INTRODUCTION

ANTENNA diversity for land-mobile radio base stations is very effective [1]. In fact, spatial diversity with receive antennas spaced typically ten or more wavelengths apart on cellular telephone towers is in widespread use. Recently, polarization diversity has been found to be nearly as effective as spatial diversity for base stations [2]–[4]. Thus, many operational systems are using a single polarization diversity antenna instead of two separate space diversity antennas, providing space and cost savings. Polarization diversity also compensates for polarization mismatch due to random handset orientation [5]. Pattern diversity using multiple directional beams has also been investigated for use at base stations that have switched-beam smart antennas [6].

Spatial diversity uses two or more antennas separated in space for reception or transmission. Base-station spatial diversity requires wide antenna spacings for proper operation because the multipath arrival angle spread is narrow [1]. However, as shown in [7], under wide multipath angle spread conditions diversity spacing can be small. Wide angle spread occurs in outdoor urban and indoor environments with mobile/personal terminals.

In this paper, we present results from a major measurement campaign that demonstrates the effectiveness of spatial diversity in handsets and investigates other fundamental mechanisms that contribute to diversity gain. It was found that antenna spacings as small as one-tenth wavelength provide up to 8 dB diversity gain at a 1% outage level. Similar large gains for polarization and pattern diversity with small antenna spacings were also observed. Measurements including operator effects showed a diversity gain of over 8 dB using antennas spaced 0.25 wavelength apart with the operator's head next to the antennas. The results of this investigation can be used to design effective diversity antennas for handheld radios.

II. BACKGROUND

The basic principle of antenna diversity is that multiple antenna outputs experience different signals due to different channel conditions, and these signals are only partially correlated. Thus, it is highly likely that if one antenna is in a deep fade, then the other one is not and provides sufficient signal. In multipath propagation conditions, as encountered with a blocked or shadowed direct line-of-sight (LOS) path, each receive antenna experiences a different fading environment.

Multiple diversity dimensions can be exploited dynamically in receivers. The antenna diversity dimensions that are available are spatial (multiple antenna elements occupy separate locations on the radio), polarization (multiple antennas provide two or more different polarizations), and pattern or angle (directional antennas discriminate over angle space). It is desirable to understand the effects of varying each dimension, but in practice it is difficult to vary all three dimensions independently.

Diversity antennas provide two major benefits. First, reliability is improved in multipath channels, where interference from reflected signals causes fading of the received signal. The fade level experienced on average for a given outage probability (percent down time) is decreased through diversity. Systems that use diversity combining can provide 10 dB or more diversity gain (to be defined below) for the worst 1% of cases. Second, the overall average received signal power is increased. Systems that use polarization or angle diversity automatically adjust the antenna characteristics to produce a near maximum received signal, increasing the efficiency of the radio link. These signal increases can be dramatic. For example, a radio without polarization diversity can easily experience a 10–20 dB decrease in mean received signal power due to polarization mismatch, but with a simple polarization diversity system the worst case mismatch is 3 dB. Handheld radios that use diversity antennas have system-level benefits. Diversity systems permit the use of lower transmit power for a

Manuscript received September 20, 1999; revised December 11, 2000. This work was supported by DARPA and by Texas Instruments.

The authors are with the Virginia Tech Antenna Group, Bradley Department of Electrical and Computer Engineering, Virginia Polytechnic Institute and State University, Blacksburg, VA 24061-0111 USA (e-mail: carld@ee.vt.edu).

Publisher Item Identifier S 0018-926X(01)06374-8.

given level of reliability. This decreases interference, increases battery life of handheld radios, and reduces the probability that a hostile party will intercept the signals.

The output signals from diversity antennas can be selected or combined in several ways to optimize the received signal power or signal-to-noise ratio (SNR). These methods include selection diversity, where the signal with the higher SNR is selected, and maximal-ratio combining, in which the signals from all branches are weighted by their respective SNRs, cophased, and added. Diversity combining techniques are described in detail in [8] and [30]. Adaptive beamforming algorithms can also provide diversity gain, in addition to rejecting interfering signals [9]. In this investigation, maximal ratio combining and selection diversity are considered.

Antenna diversity is most effective in flat fading channels, which affect the signal the same way over its bandwidth. Flat fading occurs in narrow-band systems with propagation distances of up to several kilometers and in wide-band systems over indoor and pico- or microcellular channels with small delay spreads. Equalizers or RAKE receivers employed in wide-band radios cannot mitigate flat fading with a single antenna [10], but when combined with antenna diversity they can improve performance in both flat and frequency-selective fading channels.

Diversity gain quantifies the improvement in SNR of a received signal that is obtained using signals from different receiver branches. Diversity gain permits a direct comparison of improvement offered by multiple antenna sensors compared to a single one. The diversity gain for a given cumulative probability p is given by

$$G_{div}(p) = \gamma_{div}(p) - \gamma_1(p) \quad (1)$$

where γ_{div} is the SNR with diversity and γ_1 is the SNR of a single branch without diversity combining. Diversity gain is the increase in SNR, due to diversity combining, for a given level of cumulative probability or reliability.

Theoretical expressions for envelope correlation and diversity gain are used to provide a baseline for comparison with spatial diversity measurements in this paper. Diversity gain is a function of branch correlation and power imbalance and decreases as the values of those two parameters increase. In spatial diversity systems, the correlation between the branch envelopes is a function of the spacing between the antennas; the general trend is that correlation decreases with increasing antenna spacing.

Relationships among antenna spacing, branch envelope correlation, and diversity gain can be used to develop a theoretical baseline. An empirical relationship among diversity gain, branch envelope correlation, and power balance was developed by Turkmani [3]. More recently, an analytical expression for the probability density function (pdf) of the output of a maximal-ratio combiner in a Rayleigh-fading channel as a function of branch power correlation and power balance has been developed by Dietze. Schwartz *et al.* [11] derived a cumulative distribution function for the maximal-ratio combiner output, also in terms of power correlation. In this paper, diversity gain is considered as a function of power imbalance and envelope correlation, because a theoretical expression for envelope correlation as a function of antenna spacing exists. Dietze [12] has derived

the envelope correlation (ρ_e) in terms of the power correlation (ρ_P) for the correlated Rayleigh channel. The resulting expression is

$$\rho_e = \frac{E[(r_1 - \bar{r}_1)(r_2 - \bar{r}_2)]}{\sqrt{E[(r_1 - \bar{r}_1)^2]E[(r_2 - \bar{r}_2)^2]}} \\ = \frac{(1 + \sqrt{\rho_P}) E\left(\frac{2\rho_P^{1/4}}{1 + \sqrt{\rho_P}}\right) - \frac{\pi}{2}}{2 - \pi/2} \quad (2)$$

where $E(\bullet)$ is the complete elliptical integral of the second kind (under the definition of the Jacobi elliptical integral with modulus k^2) and $E[\bullet]$ is the expected value operator. The envelopes of the two diversity branches are given by r_1 and r_2 . In Ricean fading channels, fading is less severe and the potential diversity gain is lower than in the Rayleigh fading channel assumed in the theory.

Clarke [7] derived the following relationship between envelope correlation (ρ_e) and antenna separation:

$$\rho_e \cong J_0^2\left(\frac{2\pi d}{\lambda}\right) \quad (3)$$

where

- J_0 Bessel function of the first kind with order zero;
- d antenna spacing;
- λ wavelength.

This result is valid for a uniform angle of arrival distribution in azimuth and identically polarized omnidirectional receiving antennas that are matched to the polarization of the incoming wave. All multipath components are assumed to lie in the horizontal plane.

The correlation between the envelopes of signals received by two antennas is decreased if the patterns of each antenna are different; this is because the relative amplitudes of the incident multipath signals are different at each antenna, even if the antennas are collocated. The patterns of closely spaced antennas that are omnidirectional in free space are distorted due to mutual coupling. Vaughan and Scott [13] showed that envelope correlations for closely spaced monopoles were much lower than predicted by (3).

Various combinations of spatial, polarization, and pattern diversity have been considered for use at the mobile handset [13]–[26]. So far, however, little research has attempted to isolate the effects of spatial, polarization, and pattern diversity in handheld applications and considered the effect of power imbalance. This paper reports on diversity approaches used separately as well as in combination. Experiments were performed to evaluate the effects of antenna spacing, pattern, and polarization on diversity performance. The results can be valuable in guiding the configurations selected in operational systems.

III. EXPERIMENTAL CONFIGURATION

Experiments were performed using the handheld antenna array testbed (HAAT) to evaluate the performance of various diversity systems under tightly controlled conditions as well

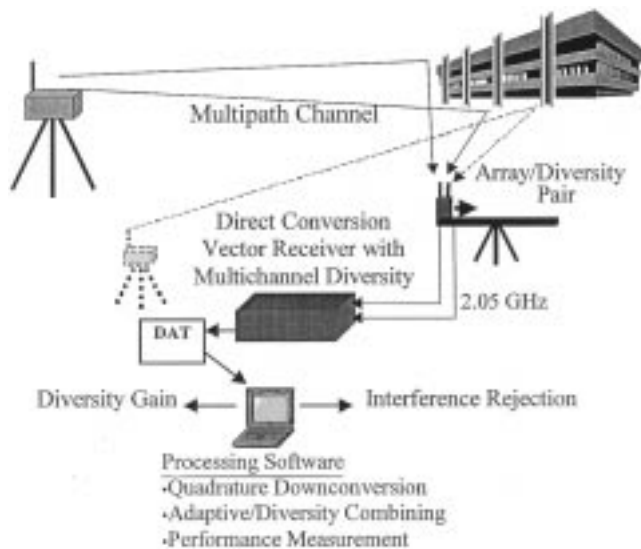


Fig. 1. Overview of the HAAT.

as in more typical operational scenarios. The HAAT is designed for maximum portability and flexibility, facilitating the data-collection process. The system is used to evaluate the performance of alternative antenna configurations and combining techniques for outdoor, indoor, and outdoor-to-indoor scenarios under LOS and NLOS conditions.

A. Handheld Antenna Array Testbed

The HAAT consists of two transmitters, a receiving system, a translating positioner for the receiver, and a data-processing system. Fig. 1 is a high-level diagram showing the components and outputs of the testbed. The frequency of 2.05 GHz was selected for relevance to PCS and PCN bands. The transmitters typically operate from a fixed position but are transportable and are powered by batteries for use in the field. The portable positioning system is used to move the receiver for controlled measurements. It consists of a nonmetallic track with a usable length of about 2.8 m (approximately 19 wavelengths at 2.05 GHz). The receiver unit is moved along the track at a constant speed of 0.115 m/s, using a stepper motor, while measurements are conducted. The track is mounted on an adjustable tripod to allow use on any terrain. Transmitter and receiver heights are approximately 1.5 m. Data are collected using the portable receiver system and analyzed offline to allow comparison of different combining techniques. In the noninterference scenarios reported in this paper, the performance measure is diversity gain. In scenarios where adaptive beamforming techniques are used to reject interfering signals, the performance measure is the improvement in signal-to-(interference plus noise) ratio (SINR) over that for a single antenna.

The receiver unit, as indicated in Fig. 1, consists of two channels, with a common local oscillator, packaged in a box that is the approximate size and shape of a handheld radio; and a portable digital audiotape (DAT) recorder, used to log data. The two received radio-frequency signals, one from each antenna, are mixed down to an audio intermediate frequency and recorded on the two channels of the stereo DAT recorder. The entire receiver unit is portable so that it can be carried by

an operator and rugged enough that it can be used to perform experiments in a wide variety of locations and conditions.

The HAAT system performance was evaluated using conventional communication link theory. Mean path loss for a distance r is given by [28]

$$PL(r) = 20 \log_{10}(4\pi r_0/\lambda) + 10n \log_{10}(r/r_0) \text{ dB} \quad (4)$$

where r , r_0 , and λ are in meters and n is the path-loss exponent (equal to two for free-space propagation) can be determined empirically for nonfree space channels. The path loss is referred to the free-space path loss at the reference distance r_0 . Each transmitter produces a 27-dBm 2.05-GHz continuous-wave signal. The receiver noise floor is approximately -88 dBm with the 100-Hz bandwidth filter that was used for processing data. Calculations using (4) with $r_0 = 1$ m yield a range of over 600 m in free space ($n = 2$) with a minimum mean SNR of 20 dB to allow for Rayleigh fading at the 1% cumulative probability level. In an obstructed channel modeled with a path-loss exponent of $n = 3$, the maximum range is 74 m. For a minimum SNR of 30 dB, allowing for Rayleigh fading at the 0.1% level, the predicted ranges for free space and for an obstructed channel are 200 and 34 m, respectively. NLOS measurements were conducted over distances of less than 50 m, while the transmitter-receiver distance was over 100 m for some of the LOS measurements and the outdoor-to-indoor measurements.

A number of parameters were varied in the controlled experiments, such as the location of the transmitter(s) and receiver, the positioner height and orientation (compass bearing). The height and angles of the transmitter and receiver antennas and antenna supports can also be adjusted. These parameters were recorded for each experiment.

B. Antenna Configurations

Many prior experiments reported in the literature offer mostly anecdotal results because the sites examined are limited in type and number and because the antennas are not fully characterized. To the extent possible, “pure” cases of spatial, polarization, and pattern diversity were used in these measurements in order to isolate the effects of each variable. This is desirable because if more than one parameter is varied, it is difficult to attribute performance change to one parameter.

The antenna configurations used for space, polarization, and pattern diversity are shown in Fig. 2. The spatial diversity configuration in Fig. 2(a) consists of two parallel half-wave dipole antennas spaced d apart; d was varied in 0.05 wavelength increments from 0.1 to 0.5 wavelength. The polarization diversity configuration of Fig. 2(b) consists of a dipole and a printed “big wheel” antenna separated vertically by 0.3λ , which was near the minimum spacing that was physically possible. The big wheel antenna [29] has an omnidirectional pattern in the horizontal plane and gain that are similar to a dipole but horizontally polarized in the azimuth plane. Thus, it has identical behavior to a dipole except for polarization. Measured co- and cross-polarized azimuth (E -plane) patterns of the big wheel antenna are shown in Fig. 3. The gain of the big wheel antenna was measured and was within 1 dB of the dipoles used in the diversity experiments. Measurements in a NLOS channel showed

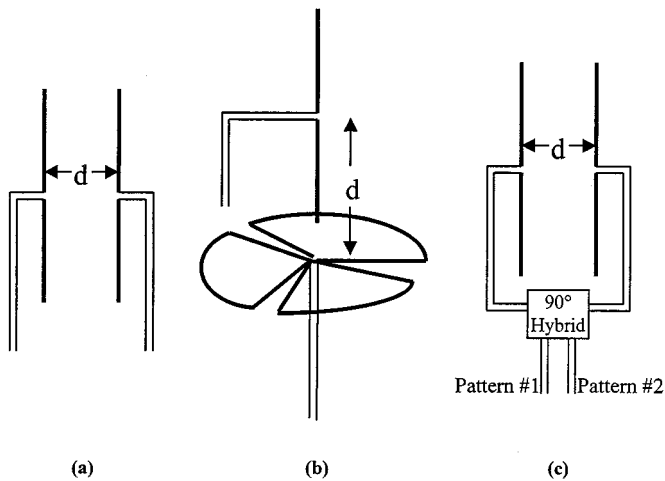


Fig. 2. Diversity antenna configurations. (a) Spatial. (b) Polarization. (c) Pattern.

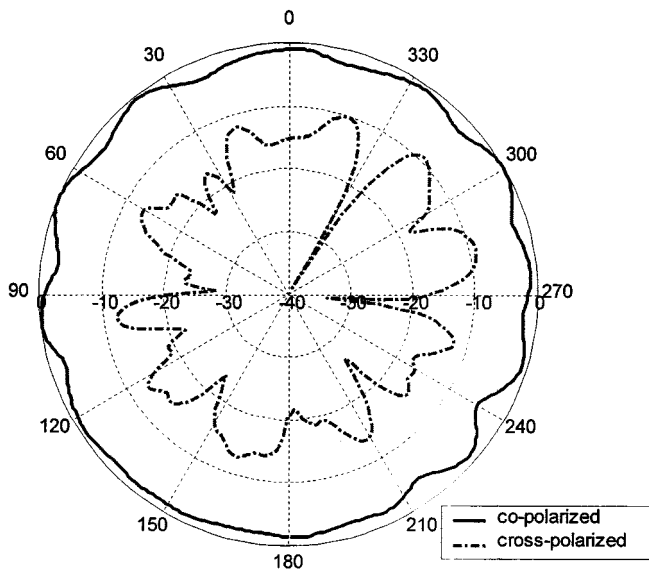


Fig. 3. Normalized measured co- and cross-polarized azimuth (E -plane) patterns for the big wheel antenna. Mean copolarized to mean cross-polarized is approximately 13 dB. Maximum copolarized to maximum cross-polarized is approximately 9 dB.

that envelope correlation decreased very gradually as the vertical spacing between the dipole and the big wheel was increased from 0.3 to 0.5λ , indicating that small variations in vertical position were not critical in this configuration. This is consistent with the assumption that multipath components are confined within a narrow range of elevation angles about horizontal. If this assumption holds, the decorrelation between the signals received by the dipole and the big wheel is primarily due to the difference in antenna polarizations. One set of polarization diversity experiments was performed prior to the construction of the big wheel antennas and used two crossed (vertical and horizontal) half-wave dipoles. Pattern diversity measurements used two dipoles connected to a 90° hybrid, as shown in Fig. 2(c), with d fixed at 0.25λ . This yielded two (ideally orthogonal) directional patterns with opposing beam maxima directions. The measured patterns and patterns obtained with a moment method model are shown in Fig. 4.

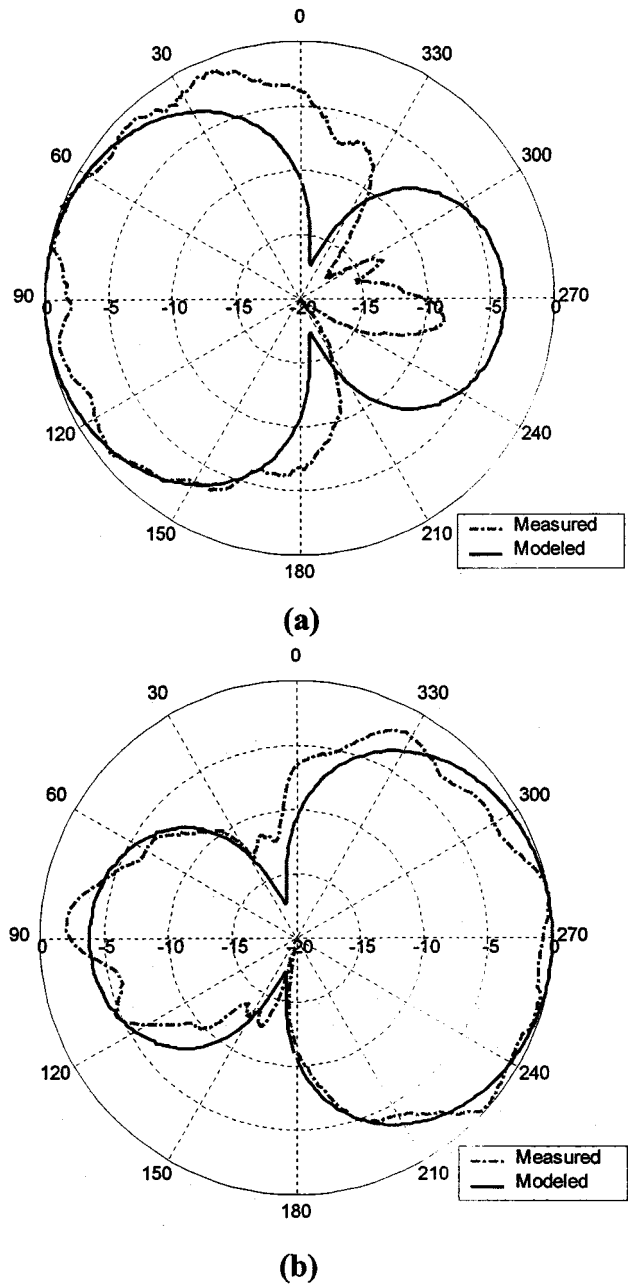


Fig. 4. Normalized measured and modeled patterns for the pattern diversity antenna configuration of Fig. 2(c) with antenna spacing $d = 0.25$ wavelength: (a) pattern 1 and (b) pattern 2.

A single transmitter was used in each set of diversity experiments. The transmitter used a half-wave dipole antenna that was oriented vertically for spatial and pattern diversity measurements. The dipole was oriented 45° from vertical, in a plane normal to the transmitter–receiver line, for polarization diversity measurements.

C. Mutual Coupling

The effects of mutual coupling change the antenna patterns from the free-space pattern. In the case of spatial diversity in particular, the change in patterns tends to decrease the correlation between two closely spaced antennas below the theoretical value [13]. This is because the expression in (3) was calculated assuming omnidirectional patterns. In a practical system, each

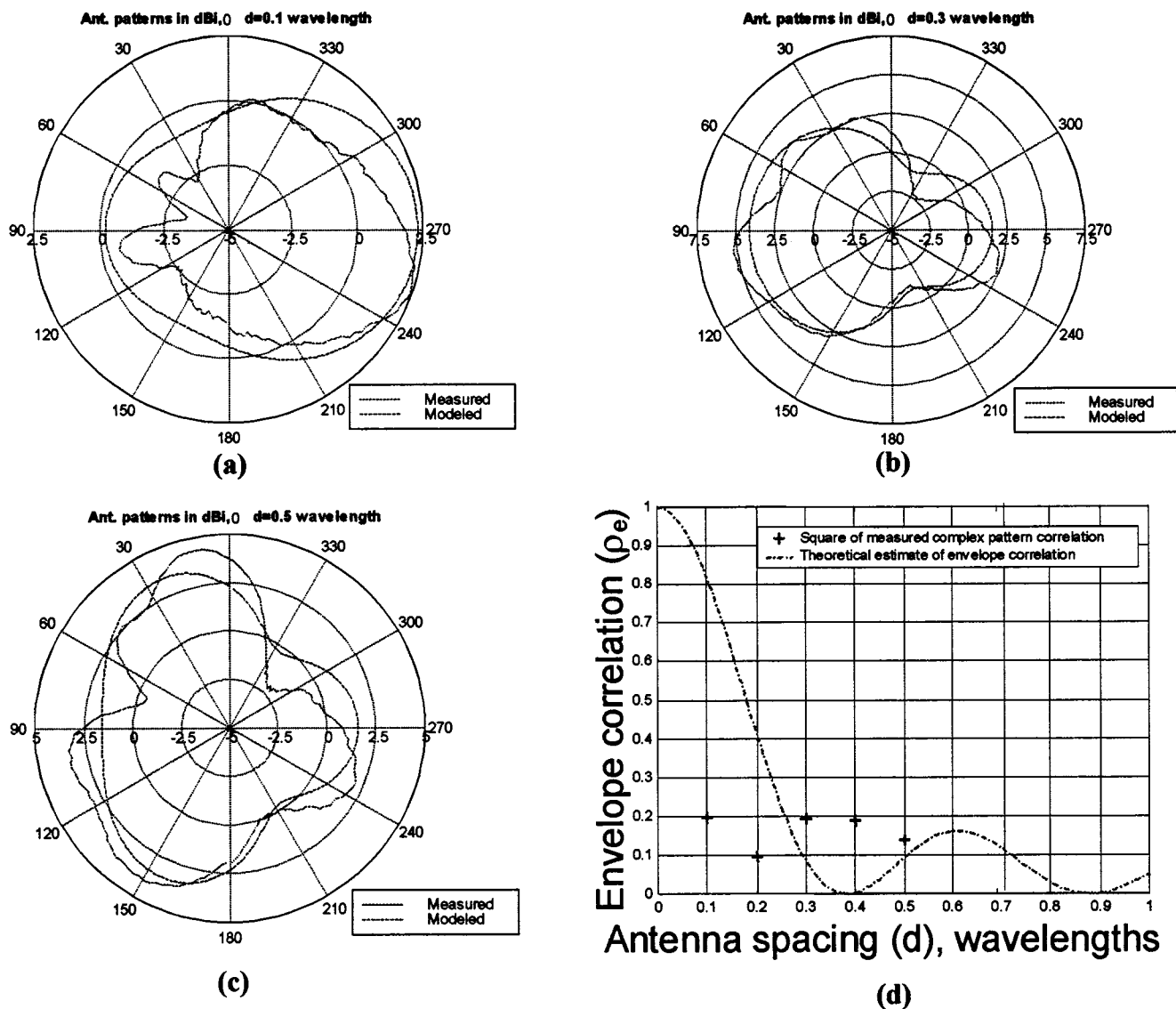


Fig. 5. Effects of mutual coupling. (a) Azimuth pattern of dipole with 0.1λ spacing. (b) Azimuth pattern of dipole with 0.3λ spacing. (c) Azimuth pattern of dipole with 0.5λ spacing. (d) Squared correlation of complex pattern versus spacing, measured, and theoretical for omnidirectional patterns.

antenna has a different pattern due to pattern distortion caused by mutual coupling. Therefore, the relative weights of incoming multipath components received by each antenna are different, even when the antennas are closely spaced and the phases of the multipath components received by each antenna are similar. This reduces the probability that the received signals at both antennas will fade simultaneously. To investigate the pattern effects of mutual coupling, patterns of each dipole in the spatial diversity configuration of Fig. 2(a) were measured on an outdoor range with the first dipole centered over the positioner. The pattern of each diversity antenna was measured for spacings from 0.1 to 0.5λ . Fig. 5(a)–(c) shows measured copolarized azimuth (H -plane) patterns of one dipole for spacings of 0.1 , 0.3 , and 0.5λ , respectively, with the other dipole terminated. The patterns calculated using the NEC moment method simulation code are included in Fig. 5 and agree closely with the measured patterns. The slight asymmetry in the measured patterns is probably due to the antenna feeds, which were not modeled.

If the antennas had pure omnidirectional patterns, the square of the correlation of the complex antenna patterns over azimuth angle would vary as a squared Bessel function of the electrical antenna spacing. This coincides with the function for the envelope correlation from (3). Fig. 5(d) shows that the squared correlations of the complex patterns are generally lower than the theoretical curve, especially for small spacings. This is because the measured patterns include the effects of pattern distortion due to mutual coupling as well as the effects of antenna spacing on the phase of the received signal.

Mutual coupling also has a significant effect on the pattern diversity configuration. The patterns shown in Fig. 4, obtained with the configuration of Fig. 2(c), do not coincide with the cardioid pattern predicted by array theory for omnidirectional element patterns but agree closely with the NEC model of this antenna configuration. The patterns are directional with opposing maxima and a front-to-back ratio of approximately 4 dB (modeled) and 2 and 9 dB (measured).

D. Measurement Cases

Controlled experiments were conducted using the HAAT in urban, "urban canyon," suburban, and rural locations that varied from flat to mountainous terrain, including both LOS and NLOS (shadowed) channels. A single transmitter was used in these experiments. The receiver was mounted on the linear positioner, and received data were recorded as the receiver moved along the 2.8 m track. Four measurement runs were performed for each antenna configuration, and the track was rotated 45° in azimuth between measurement run sectors to yield representative statistics from all directions (the antenna configurations were symmetric about the positioner axis). The symmetry of statistics for measurements separated by 180° was confirmed for an urban NLOS channel. Transmitter and receiver antenna heights were approximately 1.5 m, representing a peer-to-peer scenario.

An additional set of measurements was performed with and without an operator's head in close proximity to the receiving antennas, with the operator walking alongside the unit as it moved down the track. These measurements were taken in an urban NLOS location and consisted of eight measurements with the operator and eight measurements without the operator, with the track rotated 45° between measurements. It was necessary to cover the full 360° in azimuth because the operator disrupted the symmetry of the system.

E. Repeatability of Measurements

Repeated measurements over the same track were performed in an indoor controlled environment to test for repeatability. The correlation of the envelopes recorded in successive runs was 0.98. In outdoor measurements with pedestrian traffic, correlations as high as 0.94 were observed between repeated runs. Even when the correlation was lower, the envelope correlation, power imbalance, and diversity gain for repeated measurements were very similar.

IV. DATA PROCESSING

Data collected with the HAAT were processed offline. This has the advantage of allowing comparison of different diversity combining techniques. It is also possible to reprocess the data using new algorithms or to calculate other statistics from these data in the future. The data-processing system consists of a computer with an interface to the data logger and software that determines statistics of the collected data and evaluates the performance of different combining techniques for each antenna configuration tested. For diversity combining, the statistics of most interest are diversity gain, envelope correlation, and power imbalance, where diversity gain is the most relevant to system performance. The Ricean parameter K is also calculated. Data are recorded from the DAT using a digital audio card and stored in files on a computer using a sampling rate of 32 kHz, two channels, and 16 bits per sample. In this format, 1 min of data occupies approximately 10 MB of disk space. The data-processing software reads the data files and processes the data to determine the statistics of the data and the performance of combining techniques. The signal-to-noise ratio after maximal ratio, equal gain, and selection diversity are calculated

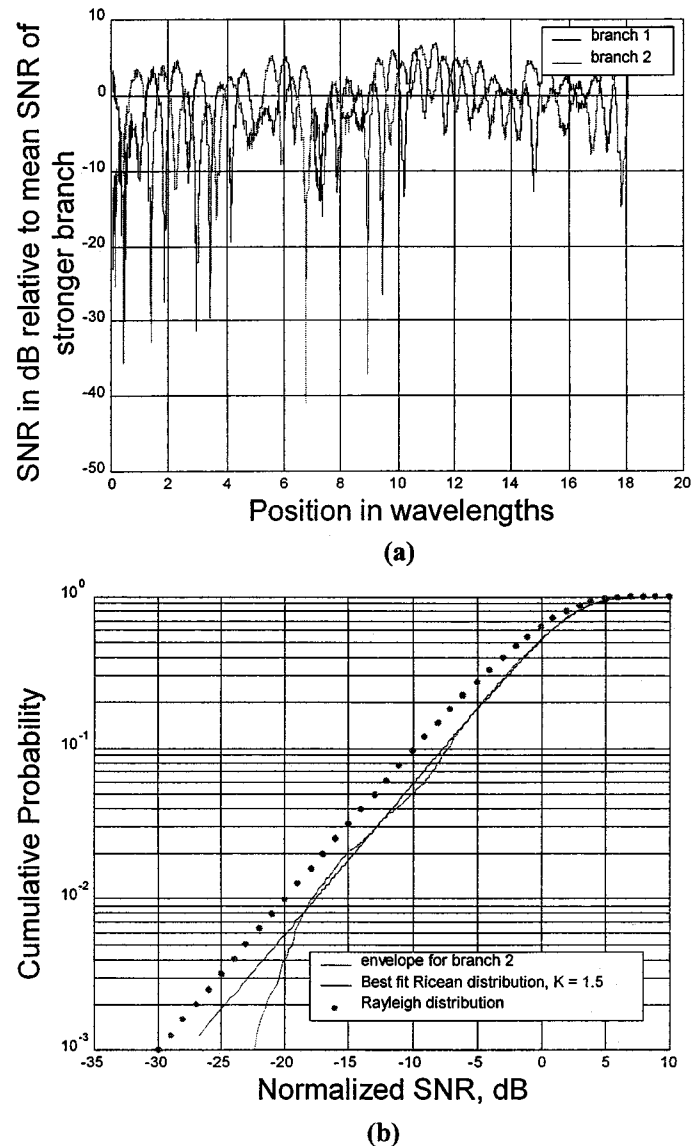


Fig. 6. (a) Signal envelope as a function of terminal position in an urban NLOS channel. (b) cdf of signal envelope with best fit Ricean cdf, $K = 1.5$.

based on expressions given in [11]. Each measurement is processed, and then measurement sets are processed based on information specified in a measurement set description file. The program calculates statistics for each antenna spacing used in the measurement set. The calculated statistics include the mean of the envelope correlation, the mean absolute power imbalance, the mean power imbalance ($\mu_{|\Delta P|}$), and the mean diversity gain for measurements using each antenna spacing. For spatial diversity measurements, a range of antenna spacings are used, while for polarization and pattern diversity measurements, typically only one antenna spacing is used.

Demeaning, or removal of the local mean of the fading envelope, is sometimes used by researchers to remove the effects of shadowing from the data, but this is not readily applicable to the measurements presented here because shadowing tends to remain nearly constant over short distances. Demeaning using a six-wavelength window (as in [26]) reduced the envelope correlation from about 0.3 to 0.2 for NLOS cases and from 0.6 to

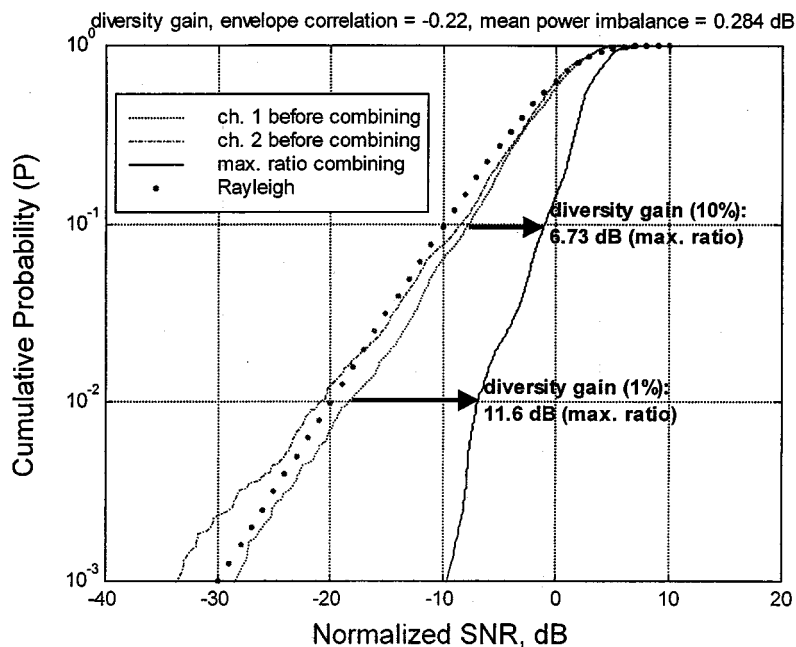


Fig. 7. Cumulative distribution function of signals before and after diversity combining, showing diversity gain, for an urban NLOS measurement.

0.4 for LOS cases (where no shadowing was present and demeaning is clearly not appropriate). Demeaning changed the diversity gain by less than 1 dB in most cases. It was determined that demeaning was not necessary or appropriate for these measurements, so all results are presented for data processed without demeaning.

As stated previously, power balance is important for determining the diversity gain of a system. It is essential that this information is not lost in the data processing. To accomplish this, the envelopes of both branches are normalized to the mean of the stronger branch. This approach yields envelopes that are normalized relative to a common reference and preserves the power balance information. Fig. 6(a) shows measured signal envelopes in an urban NLOS channel.

The probability distribution of the envelope in a fading channel can be characterized by a Ricean distribution. For each measurement, the Ricean parameter K (the specular-to-random power ratio) is found that yields a best fit to the normalized cumulative distribution function (cdf) of the measured envelope for each channel. K is calculated in increments of 0.1. A channel that has only multipath with no dominant path will have a value of $K = 0$ (Rayleigh fading). An example of a best fit Ricean cdf for an urban NLOS channel is shown in Fig. 6(b), where $K = 1.5$. This corresponds to the theoretical fading distribution for a received signal with one dominant component that has approximately 1.5 times the total power of all the other multipath components. Knowledge of the fading distribution allows us to determine whether the measured diversity gain should be expected to approach the theoretical diversity gain for Rayleigh fading.

Diversity gain was calculated based on the envelope levels assuming equal noise power in each branch using (1). CDFs are shown in Fig. 7 for the envelopes of the signals received by each diversity branch, as well as for the calculated envelope of the signal after maximal ratio combining. The CDFs are normalized

to the time average of the stronger branch. The diversity gain for a given cumulative probability (read from the y -axis) is the horizontal distance between the curve for the stronger branch (channel 1 in this case) and the curve for the combined signal. For example, the diversity gain from Fig. 7 is approximately 6.7 dB for 10% cumulative probability and 11.6 dB for a 1% cumulative probability.

V. EXPERIMENTAL RESULTS

Measurements were divided into four categories so that measurement sets within a group represented similar types of channels and had generally similar statistics. As shown in Table I, these categories are LOS (urban and suburban), NLOS (urban and rural), urban canyon (NLOS between rows of buildings), and indoor and outdoor-to-indoor. First, we discuss the results of the spatial diversity measurements, and then polarization and pattern diversity measurements.

Fig. 8 shows the envelope correlations from the spatial diversity measurements. The measured correlations are below the theoretical curve for small antenna spacings and above the curve for spacings larger than about 0.2 wavelength. The correlation for all spacings is below 0.7, which is typically considered to be the maximum for effective diversity combining. The correlation for the urban canyon channels is highest, probably because the multipath angle spread is relatively small. For LOS measurements, the receiver and transmitter were surrounded by buildings and the multipath angle spread is large, although the LOS component should dominate. For the indoor and outdoor-to-indoor measurements, the fading approaches the Rayleigh distribution, and multipath can be expected to be more evenly distributed than in the other cases. This results in low envelope correlations for spatial diversity configurations in the indoor and outdoor-to-indoor channels.

TABLE I
CATEGORIES OF MEASUREMENT SETS WITH STATISTICS OF THE MEASUREMENT SET MEAN VALUES. G_{div} IS THE DIVERSITY GAIN AT THE 99% RELIABILITY LEVEL WITH MAXIMAL RATIO COMBINING

	K		ρ_e		G_{div}	
	μ	σ	μ	σ	μ	σ
Line-of-sight (LOS)	1.86	0.22	0.42	0.04	6.44	0.15
Non line-of-sight (NLOS)	1.16	0.58	0.36	0.09	8.81	0.75
Urban Canyon, non line-of-sight (UCN)	1.29	0.26	0.6	0.03	7.43	0.4
Indoor and Outdoor-to-indoor (I, OI)	0.63	0.08	0.27	0.22	8.57	0.41

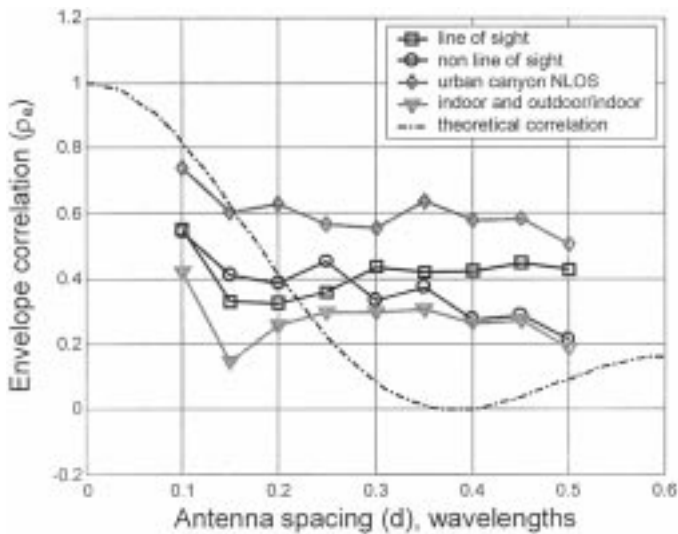


Fig. 8. Envelope correlations as a function of antenna spacing for LOS, NLOS, urban canyon, and outdoor-to-indoor/indoor channels.

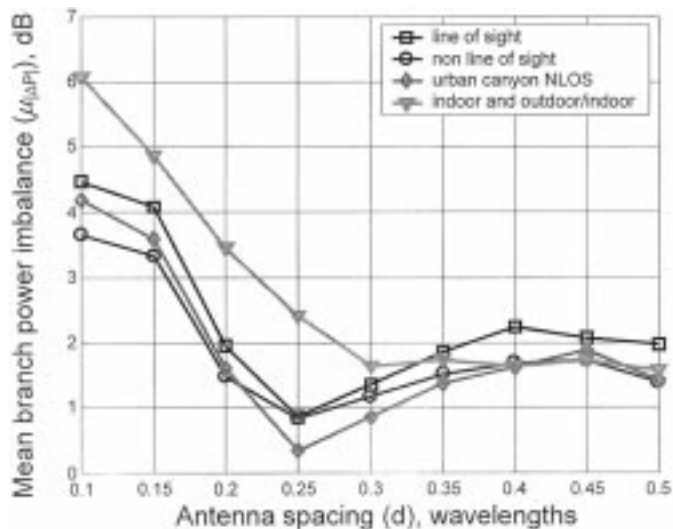
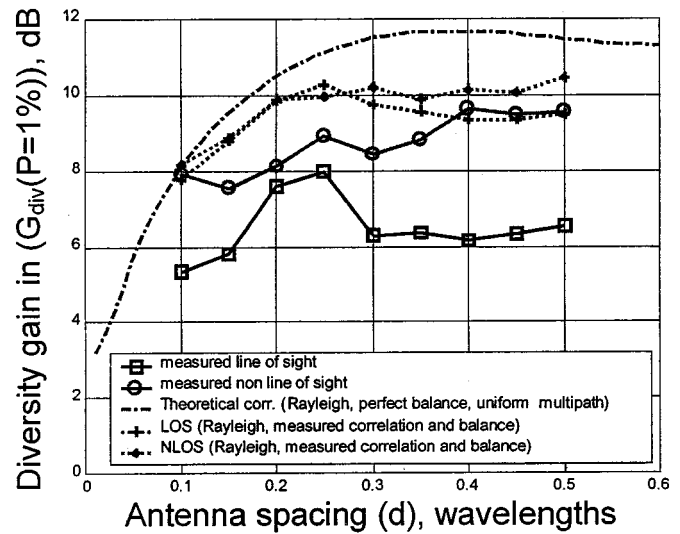
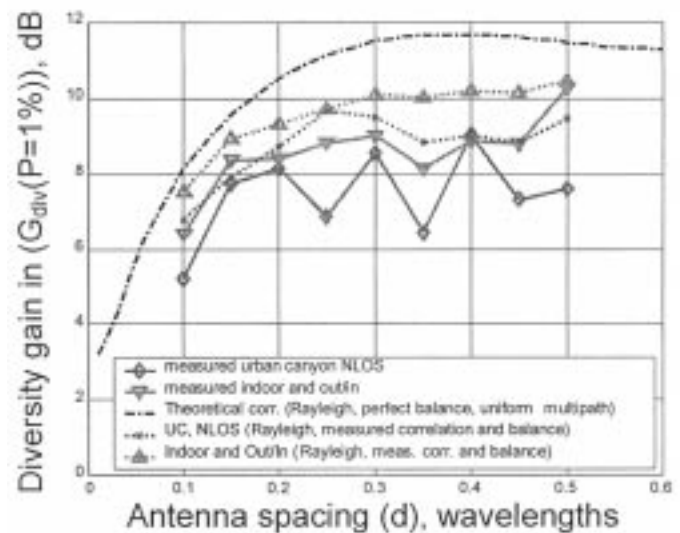


Fig. 9. Branch power imbalance versus antenna spacing.

Power balance varied as a function of antenna spacing and ranged from 0.5 to 6 dB, as shown in Fig. 9. The statistics for all types of channels were similar, and the values of power imbalance were relatively large. This suggests that the assumption of perfectly uniform angular distribution of multipath, which was used to derive (3) and which would result in 0 dB imbalance, is not satisfied for any of the channels. However, for spacings greater than 0.2λ , power imbalance is usually less than 2 dB.



(a)



(b)

Fig. 10. Diversity gain as a function of antenna spacing for (a) outdoor LOS and NLOS and (b) urban canyon and indoor-to-outdoor/indoor measurements.

Fig. 10 shows the calculated diversity gain, averaged over four measurement runs for each antenna spacing, for maximal ratio combining at the 1% cumulative probability or 99% reliability level. The ideal theoretical curve is obtained using Dietze's expression for the maximal-ratio combiner output pdf with the envelope correlations given by (3) for perfect power balance. The other theoretical curves are calculated using the

TABLE II
STATISTICS FOR EACH MEASUREMENT LOCATION

Antenna Configuration	Channel	Ricean Parameter K	Envelope correlation	Power imbalance, dB	Div. gain in dB with max. ratio, 99% reliability	Div. gain in dB with selection, 99% reliability
Spatial	NLOS1*	1.00	0.12 – 0.56	0.9 – 2.5	8.9 – 10.3	7.5 – 8.9
	NLOS1A*	0.70	0.12 – 0.49	0.7 – 4.4	7.4 – 10.4	6.0 – 9.0
	NLOS2*	2.01	0.27 – 0.72	0.6 – 3.8	6.4 – 9.9	4.7 – 8.3
	UCN1*	1.10	0.50 – 0.74	0.4 – 4.5	5.6 – 9.6	4.1 – 8.2
	UCN2*	1.47	0.45 – 0.74	0.3 – 3.8	4.7 – 8.3	3.3 – 7.0
	NLOS3 [†]	0.92	0.29 – 0.60	1.2 – 3.9	6.2 – 10.6	4.6 – 9.0
	LOS1**	1.95	0.38 – 0.56	1.1 – 3.7	4.5 – 7.7	2.9 – 6.0
	LOS2*	2.03	0.23 – 0.48	0.3 – 6.1	4.9 – 8.2	3.1 – 6.5
	LOS3**	1.61	0.30 – 0.69	1.4 – 3.9	4.7 – 7.7	3.2 – 6.1
	OI ^{††}	0.68	0.36 – 0.52	1.2 – 5.9	6.1 – 11.3	4.8 – 10.0
I [‡]	0.57	-0.67 – 0.42	1.6 – 6.2	6.7 – 9.3	5.5 – 7.8	
Polarization	NLOS1A*	0.79	-0.013	3.1	9.2	7.8
	NLOS3 [†]	1.15	-0.052	5.2	8.6	6.8
	UCN1*	1.10	0.26	6.7	6.8	5.3
	UCN2*	1.32	0.12	13.0	3.3	1.9
	LOS1***	1.48	0.03 – 0.39	4.3 – 4.8	5.5 – 8.7	4.1 – 7.0
	LOS2*	2.06	0.23	3.8	6.3	4.5
	LOS3**	1.45	0.17	8.4	3.9	2.1
	OI ^{††}	0.69	0.34	1.5	9.5	8.0
	I [‡]	0.44	0.07	1.5	10.6	9.5
	Pattern	NLOS1A*	1.20	-0.13 – 0.08	5.6 – 6.2	9.2 – 11.2
NLOS3 [†]		0.98	0.12	6.7	6.5	5.3
UCN1*		1.61	0.31	7.2	6.7	5.2
UCN2*		1.33	0.32	6.5	7.8	6.1
LOS2*		2.40	0.22	6.0	3.8	1.7
LOS3**		1.40	0.19	7.1	4.8	3.7
OI ^{††}		0.58	0.17	5.2	8.9	7.2
I [‡]		0.43	0.02	2.3	7.6	6.0

* Urban, ** Suburban, [†] Rural, ^{††} Outdoor-to-Indoor, [‡] Indoor, ^{‡‡} Crossed dipoles

measured envelope correlations and power imbalances. This results in an estimate of diversity gain that is up to 5 dB lower (for urban canyon and LOS) or up to 4 dB lower (for NLOS and indoor/outdoor-to-indoor) than the estimate using the theoretical correlation and perfect power balance. The measured results compare more closely to the more conservative theoretical estimate of diversity gain calculated for a maximal-ratio combiner using the measured envelope correlations and power imbalance. The maximal-ratio combiner output is calculated for Rayleigh fading, which was not exactly representative of any of the measured channels. The mean value of the Ricean specular-to-random ratio K for the measured channels ranged from 0.57 to 2.03; $K = 0$, for Rayleigh fading. As a result, the theoretical predicted diversity gain is overly optimistic for the channel conditions. The measured diversity gain for antenna spacings of 0.2λ or more is substantial even though it is less than the theoretical prediction; it is greater than 8 dB for NLOS nonurban canyon channels.

Results of measurements using spatial, polarization, and pattern diversity configurations are summarized in Table II, categorized by diversity configuration. It can be seen that 7–10 dB diversity gain at the 1% probability (99% reliability) level is typical for spatial diversity with maximal ratio combining in the NLOS channels that were measured. Comparable gains of

6–11 dB were obtained using polarization and pattern diversity, with small antenna spacings of 0.25–0.3 wavelength. Diversity gains calculated for selection diversity were typically about 1.5 dB lower than those for maximal ratio combining for all antenna configurations.

Polarization diversity configurations have the advantage over spatial diversity of providing gain in LOS channels with very little multipath. Polarization mismatches of up to 12 dB or more were observed when transmit and receive antennas were oriented orthogonally. This problem sometimes occurs in operational systems, where handset orientation is random. Polarization mismatch is eliminated when polarization diversity is used.

Table III shows results of some additional measurements that were part of data set NLOS1A. A spatial diversity configuration using dipoles spaced 0.25λ apart was tested with and without a person's head next to the receiver antennas. The person walked along with the receiver unit as it was moved on the linear positioner. The presence of a human head increased the envelope correlation and power imbalance and decreased the diversity gain by about 2 dB. Still, a substantial diversity gain of 8.8 dB was calculated at the 99% reliability level. It is likely that the operator's head blocks some of the multipath components and reduces the effective angular spread of the received multipath components, thus increasing the envelope correlation and

TABLE III
STATISTICS FOR SPATIAL DIVERSITY MEASUREMENT (WITH AND WITHOUT OPERATOR'S HEAD PRESENT, VERTICAL DIPOLES WITH $d = 0.25\lambda$)

	envelope correlation	power imbalance	diversity gain with maximum ratio, 99% reliability	diversity gain with selection diversity, 99% reliability
without operator	0.31	0.4 dB	10.6 dB	9.4 dB
with operator	0.44	0.5 dB	8.8 dB	7.1 dB

reducing diversity gain. These results depend on a number of factors, so caution should be exercised when using the values from this one set of measurements.

VI. CONCLUSION

Spatial, polarization, and pattern diversity configurations were measured in a variety of channels including LOS, NLOS, urban, suburban, rural, urban canyon, and indoor channels. These channels exhibited fading that was approximately Ricean, with mean values of specular-to-random power ratio K that range from approximately 0.6 to 2.0. Although complete separation of spatial, polarization, and pattern effects is not possible because of antenna interactions and practical difficulties in colocating antennas, this paper provides a comparison of different configurations, each of which relies primarily on one diversity mechanism. Envelope correlations below 0.7 were observed in all channels by all spatial, polarization, and pattern diversity configurations that had spacings greater than 0.1 wavelengths. This investigation showed that diversity gains of 7–10 dB can be achieved at the 99% reliability level using spatial, polarization, or pattern diversity. Diversity gain of 8 to 9 dB is typical in NLOS indoor and outdoor channels. These gains can be achieved with antenna spacings as small as $0.1\text{--}0.15\lambda$. The measurements indicate that polarization diversity configurations can increase SNR by 12 dB or more in certain cases by eliminating polarization mismatch.

As reported in [13], envelope correlation for spatial diversity configurations was lower than predicted by simple theory, resulting in (3). This effect is caused by distortion of the individual antenna patterns due to mutual coupling and nonuniformity in the multipath angle of arrival. The effects of mutual coupling are not entirely beneficial, since the distorted patterns also cause power imbalance if the multipath is not uniformly distributed in angle. This reduces diversity gain compared to the gain that can be achieved using omnidirectional elements with a similar correlation coefficient. This can be seen in comparisons of diversity gain calculated using Dietze's expression with theoretical and measured values for the correlation and power balance.

The measurements reported here were for narrow-band signals. When operated in frequency-flat fading environments, wide-band radios should experience benefits from diversity combining similar to those seen by narrow-band systems. Wide-band systems that operate in frequency-selective fading environments are likely to require different approaches, such as adaptive arrays consisting of three or more elements or diversity combining that includes some form of temporal processing.

Wide-band experiments are planned to measure channel characteristics and performance of narrow- and wide-band combining approaches for diversity reception of wide-band signals in channels with varying temporal characteristics.

ACKNOWLEDGMENT

The authors thank K. Takamizawa, B.-K. Kim, M.-C. Huynh, R. Ertel, and R. Mostafa for assistance in measuring antenna patterns and verifying operation of the HAAT system.

REFERENCES

- [1] W. C. Y. Lee, "Antenna spacing requirement for a mobile radio base-station diversity," *Bell Syst. Tech. J.*, vol. 50, pp. 1859–1876, July/Aug. 1971.
- [2] W. C. Y. Lee and Y. S. Yeh, "Polarization diversity for mobile radio," *IEEE Trans. Commun.*, vol. COM-20, pp. 912–923, May 1972.
- [3] A. M. D. Turkmani, A. A. Arowojolu, P. A. Jefford, and C. J. Kellet, "An experimental evaluation of the performance of two-branch space and polarization diversity schemes at 1800 MHz," *IEEE Trans. Veh. Technol.*, vol. 44, pp. 318–326, Mar. 1995.
- [4] F. Lotse, J.-E. Berg, U. Forseen, and P. Idahl, "Base station polarization diversity reception in macrocellular systems at 1800 MHz," in *Proc. 46th Veh. Tech. Conf.*, vol. 3, 1996, pp. 1643–1646.
- [5] D. C. Cox, "Antenna diversity performance in mitigating the effects of portable radio telephone orientation and multipath propagation," *IEEE Trans. Commun.*, vol. COM-31, pp. 620–628, May 1983.
- [6] P. L. Perini and C. L. Holloway, "Angle and space diversity comparisons in different mobile radio environments," *IEEE Trans. Antennas Propag.*, vol. 46, pp. 764–775, June 1998.
- [7] R. H. Clarke, "A statistical theory of mobile-radio reception," *Bell Syst. Tech. J.*, pp. 957–1000, July–Aug. 1968.
- [8] W. C. Jakes, Ed., *Microwave Mobile Communications*. New York: Wiley, 1974.
- [9] J. H. Winters, J. Salz, and R. D. Gitlin, "Adaptive antennas for digital mobile radio," in *Proc. IEEE Long Island Section Adaptive Antenna Systems Symp.*, Long Island, Nov. 19, 1992, pp. 81–86.
- [10] N. Benvenuto and L. Tomba, "Performance comparison of space diversity and equalization techniques for indoor radio systems," *IEEE Trans. Veh. Technol.*, vol. 46, pp. 358–368, May 1997.
- [11] M. Schwartz, W. R. Bennet, and S. Stein, *Communication Systems and Techniques*. New York: McGraw-Hill, 1966.
- [12] K. Dietze, private communication.
- [13] R. G. Vaughan and N. L. Scott, "Closely spaced monopoles for mobile communications," *Radio Sci.*, vol. 28, no. 6, pp. 1259–1266, Nov.–Dec. 1993.
- [14] T. Taga and K. Tsunekawa, "A built in diversity antenna for 800 MHz band portable radio units," in *Proc. IEEE APS Symp.*, 1986, pp. 705–708.
- [15] K. Tsunekawa, "Diversity antennas for portable telephones," in *Proc. IEEE Veh. Tech. Conf.*, 1989, pp. 50–56.
- [16] T. Taga, "Characteristics of space-diversity branch using parallel dipole antennas in mobile radio communications," *Electron. Commun. Jpn.*, pt. 1, vol. 76, no. 9, pp. 55–65, 1993.
- [17] K. Tsunekawa and K. Kagoshima, "Diversity performance analysis of two parallel dipole antennas mounted on a small metal body," *Electron. Commun. Jpn.*, pt. 1, vol. 76, no. 10, pp. 80–90, 1993.
- [18] K. Ogawa and T. Uwano, "A diversity antenna for very small 800 MHz band portable telephones," *IEEE Trans. Antennas Propag.*, pp. 1342–1345, Sept. 1994.

- [19] S. Mano, M. Kimata, N. Inagaki, and N. Kikuma, "Application of planar multibeam array antennas to diversity reception," *Electron. Commun. Jpn.*, pt. 1, vol. 79, no. 11, pp. 104–112, 1996.
- [20] G. Dolmans and L. Leyten, "Performance analysis of an adaptive multi-beam portable handset in fading indoor channels," in *Proc. IEEE Antennas and Propagation Society Symp.*, July 1997, pp. 342–345.
- [21] B. M. Green and M. A. Jensen, "Diversity performance of personal communications handset antennas near operator tissue," in *Proc. IEEE Antennas and Propagation Society Symp.*, July 1997, pp. 1182–1185.
- [22] M. LeFevre, M. A. Jensen, and M. D. Rice, "Indoor measurement of handset dual-antenna diversity performance," in *Proc. IEEE Veh. Technol. Conf.*, 1997.
- [23] G. Pedersen and S. Skjaeris, "Influence on antenna diversity for a hand-held phone by the presence of a person," in *Proc. IEEE Veh. Technol. Conf.*, 1997.
- [24] P. Eratuuli, P. Haapala, P. Aikio, and P. Vainikainen, "Measurements of internal handset antennas and diversity configurations with a phantom head," in *Proc. IEEE APS Symp.*, June 1998, pp. 126–129.
- [25] C. Braun, G. Engblom, and C. Beckman, "Antenna diversity for mobile telephones," in *Proc. IEEE APS Symp.*, June 1998, pp. 2220–2223.
- [26] J. S. Colburn, Y. Rahmat-Samii, M. A. Jensen, and G. J. Pottie, "Evaluation of personal communications dual-antenna handset diversity performance," *IEEE Trans. Veh. Technol.*, vol. 47, pp. 737–746, Aug. 1998.
- [27] M. G. Douglas, M. O. Okoniewski, and M. A. Stuchly, "A planar diversity antenna for hand held PCS devices," *IEEE Trans. Veh. Technol.*, vol. 47, pp. 747–754, Aug. 1998.
- [28] M. J. Feuerstein, K. L. Blackard, T. S. Rappaport, S. Y. Seidel, and H. H. Xia, "Path loss, delay spread, and outage models as functions of antenna height for microcellular system design," *IEEE Trans. Veh. Technol.*, vol. 43, Aug. 1994.
- [29] *The A.R.R.L. Antenna Book*, 10th ed. Newington, CT: American Radio Relay League, Inc., 1964, pp. 318–320.
- [30] W. C. Jakes, Ed., *Microwave Mobile Communications*. New York: IEEE Press, 1993.



Carl B. Dietrich, Jr. (S'86–M'87) received the B.S.E.E. degree from Texas A&M University, College Station, and the M.S. and Ph.D. degrees in electrical engineering from Virginia Polytechnic Institute and State University, Blacksburg (Virginia Tech).

He is a Research Associate in the Virginia Tech Antenna Group. His research interests include adaptive arrays and diversity systems for reliable wireless communications. He has been with Bell Northern Research and the Defense Information Systems Agency.



Kai Dietze received the Bachelor's degree in electrical engineering from Michigan Technological University, Houghton. He is currently pursuing the Ph.D. degree in the Bradley Department of Electrical Engineering, Virginia Polytechnic Institute and State University (Virginia Tech), Blacksburg.

He is a Research Assistant in the Virginia Tech Antenna Group. His research interests are in wireless communications, primarily in the areas of adaptive antenna arrays and diversity systems.

J. Randall Nealy was born in South Carolina. He received the B.S. degree in electrical engineering from Clemson University, Clemson, SC.

Since 1989, he has been with Virginia Polytechnic Institute and State University (Virginia Tech), Blacksburg, as an Engineer for the Satellite Communications Group and the Virginia Tech Antenna Group (VTAG). At Virginia Tech, he supervised construction of microwave receivers for the NASA-sponsored ACTS and Olympus satellite propagation projects. While working with VTAG, he participated in the development of new antenna range system (Range Runner) and the new 30-in indoor tapered antenna range. He has received three U.S. patents for novel antenna designs.



Warren L. Stutzman (S'63–M'69–SM'77–F'89) received the B.S. degree in electrical engineering and the A.B. degree in mathematics from the University of Illinois, Urbana, in 1964 and the M.S. and Ph.D. degrees in electrical engineering from The Ohio State University, Columbus, in 1965 and 1969, respectively.

In 1969, he joined the Bradley Department of Electrical and Computer Engineering, Virginia Polytechnic Institute and State University (Virginia Tech), Blacksburg, where he is currently the Interim Department Head and the Thomas Phillips Professor of Engineering. He is Director of the Virginia Tech Antenna Group, which is part of the Center for Wireless Telecommunications. In 1983, he was a Visiting Professor at the Physical Science Laboratory of New Mexico State University. He works in several areas of antennas and propagation. His research activities include antennas for wireless, wide-band elements and arrays, phased array antennas, reflector antennas, personal communication systems, and atmospheric effects on earth-space communication links. He is the coauthor (with G. A. Thiele) of *Antenna Theory and Design* (New York: Wiley, 1981, 1998) and the author of *Polarization in Electromagnetic Systems* (Reading, MA: Artech House, 1993).

Dr. Stutzman was coauthor of two papers that received the Wheeler Prize for the Best Applications Paper to appear in the IEEE TRANSACTIONS ON ANTENNAS AND PROPAGATION in 1992 and 1995. He received the IEEE Third Millennium Award. He has held the following offices in the Antennas and Propagation Society: Administrative Committee from 1984 to 1986, Chairman of the AP-S Meetings Committee from 1988 to 1991, Vice President for 1991, and President for 1992.